INL/RPT-23-71239
Revision 0

ATF-2 Ramp Conceptual Design Report

February 2023

David Kamerman
Travis Labossiere-Hickman
Brian Durtschi
Gary Hoggard

Idaho National Laboratory

INL is a U.S. Department of Energy National Laboratory
operated by Battelle Energy Alliance, LLC

INL/RPT-23-71239
Revision 0

ATF-2 Ramp Conceptual Design Report

David Kamerman
Travis Labossiere-Hickman
Brian Durtschi
Gary Hoggard

February 2023

Idaho National Laboratory
Idaho Falls, Idaho 83415

http://www.inl.gov

Prepared for the
U.S. Department of Energy
Office of Nuclear Energy
Under DOE Idaho Operations Office
Contract DE-AC07-05ID14517

Page intentionally left blank

ABSTRACT

The following report documents the conceptual design for the ATF-2 Ramp experiment. The experiment aims to fill the in-pile irradiation testing gap to conduct integral ramp testing, which was created by the closure of R2, Osiris, and Halden test reactors. The concept involves the simultaneous ramping of three fuel pins using a power axial locator mechanism in the Loop-2A testing facility in the center flux trap of the advanced test reactor (ATR). The three fuel pins are ramped in individual coolant channels containing a prototypic PWR environment. Rod failure will be detected using a fuel rod elongation sensor attached to the fuel pin upper end cap. An axial stack of concentric hafnium and zirconium shrouds will be used to shape the flux around the test pins to create different power levels in each pin and to ensure the peak power location of each pin remains in the center of the test rod. Monte Carlo simulations are used to demonstrate the viability of this design concept.

Page intentionally left blank

CONTENTS

FIGURES

TABLES

ACRONYMS

ATF	Accident tolerant fuel
ATR	Advanced Test Reactor
CP	conditioning power
FGR	fission gas released
LHGR	linear heat generation rate
LVDT	linear variable differential transducer
LWR	light water reactor
MCNP	Monte Carlo N-Particle Transport Code
PALM	power axial locator mechanism
PCI	pellet cladding interaction
PWR	pressurized water reactor
RTP	ramp terminal power

Page intentionally left blank

ATF-2 Ramp Conceptual Design Report

1. MOTIVATION AND BACKGROUND

The purpose of the Accident Tolerant Fuel 2 (ATF-2) ramp experiment is to conduct pellet cladding interaction (PCI) power ramp tests in the center flux trap of the Advanced Test Reactor (ATR) during ATR's transient power cycles. The tests would run concurrently with the existing ATF-2 campaign and would not displace the ATF-2 campaign as they would occur in transient power cycles in ATR when the current ATF-2 test is not operated. PCI power ramp tests involve irradiating a light water reactor (LWR) test pin at a low-to-moderate conditioning power level (CP), usually around 200 w/cm for at least 12 hours and then increasing the power in the test pins to a ramp terminal power level and holding at the ramp terminal power (RTP) level for at least 12 more hours. Generally, ramp rates are in in the range of 100 W/cm-min with RTP levels ranging from 400 w/cm to over 600 w/cm. At times the ramps can be conducted in a "staircase" fashion with intermediate hold points between the CP and the RTP.

The tests are designed to mimic the behavior of LWR fuel rods, which see a rise in power due to changes in reactor power, movement of a nearby control element, the burnout of a burnable poison, or the movement of the fuel bundle between different locations in the core after its first or second cycle of irradiation. During irradiation of a standard LWR fuel pin with zirconium alloy cladding and oxide fuel pellets, the cladding and fuel come into mechanical contact as the result of cladding creep down and pellet swelling. When the fuel pin is then operated at a considerably higher power than what the fuel rod has been conditioned at, the expansion of the pellet causes a multi-axial tensile stress in the cladding. Radial cracks in the fuel pellet can cause a stress concentration where the crack interfaces with the inside of the cladding. Corrosive fission gases such as iodine can also be released from the pellet during the power ramp and lead to stress corrosion cracking in the cladding. These cracks can lead to a cladding breach and result in a failure of the cladding to provide a hermetic boundary between the reactor coolant and the fuel pellet.

Early PCI ramp testing was conducted with the aim of determining the cladding failure limits in terms of the fuel rod burnup, ramp size, and RTP level. Later testing also focused on the gathering of fuel performance validation data such as determination of the fission gas released (FGR) to the test pin plenum during the ramp as well as the permanent hoop strain of cladding following the power ramp. Over a thousand PCI ramp tests occurred during the initial development of LWR fuel technology from the early 1970s through the middle if the last decade, principally at test reactors in Europe, such as the R2 reactor in Sweden, the Osiris reactor in France, and the Halden reactor in Norway. All three of these reactors have since been shut down and there are presently no ongoing PCI ramp testing programs in the western world.

As a result of the core damage events that occurred at the Fukushima-Daiichi nuclear power plants during the 2011 Tohoku earthquake and tsunami, the U.S. Department of Energy began the development of LWR fuel technology with enhanced accident tolerance. Technologies range from protective coatings on the zirconium alloy claddings to replacement of the zirconium alloys with iron chrome alloys or silicon carbide composite claddings. Lead test rod irradiations of the coated zirconium alloy claddings began in 2018 with the technologies showing much promise. However, no PCI ramp tests have been performed on any ATF technologies and it is unknown how these new fuel concepts will behave in PCI ramp conditions. It is anticipated that that PCI ramp performance data will be needed before any of the ATF technologies can be widely adopted by the commercial nuclear power industry. Key ramp test data needs with respect to ATF technologies are as follows:

- Precise determination of the test pin CP level, ramp rate, and RTP level
- Precise determination of the cladding temperature, determined from the test coolant conditions (temperature, pressure, and flow rate)

- Knowledge of any cladding breaches and the time of cladding breach during the test
- Knowledge of cladding deformation during the test (elongation) and after the test (permanent hoop strain)
- Knowledge of the FGR to the test pin plenum during the test in test pins which do not experience a cladding breach.

The ATF-2 ramp experiment will take place in pressurized water Loop 2A in the center flux trap of the ATR. ATR is a water-cooled plate type materials test reactor that achieved first criticality in 1967. The fuel plates are curved and arranged in a serpentine arrangement, which create nine flux traps and five independent power lobes. These loops are shown in Figure 1, which also identifies the current ATF-2 test and the fuel elements that contribute to the center lobe power. In addition to the flux traps, several experimental positions are bored out of the reactor's beryllium reflector. The reactor is approximately 1.3 meters high and 1.3 meters in diameter and is cooled with a top-down flow of pressurized water at approximately 4–5 bars of pressure and an inlet temperature of 55°C. Power in each of the four corner lobes is controlled independently by the rotation of reflector drums which do not perturb the axial power profile. A maximum power split between any of the four quadrants of 3:1. The reactor operates both normal and transient power cycles. The normal cycles consist of 60 day runs with a nominal power of ~25 MW in each lobe with limited power splits between the four quadrants. Peak flux levels during these cycles are 4e14 n/cm^2-s thermal and 2e14 n/cm^2-s fast (>1 MeV). The transient cycles last anywhere from 7–15 days with higher operating powers and wider variations between the spatial and temporal power profiles. Generally, the transient power cycles involve a 5–10 day run at a low power soak with the south lobes operated ~5 MW and the north lobes operated ~3 MW. After the low power soak, power is increased dramatically with the south lobes operating around 50 MW and the north lobes operating around 20 MW for an additional ~5 days. ATR aims to operate three concurrent steady-state cycles followed by two concurrent transient power cycles each year.

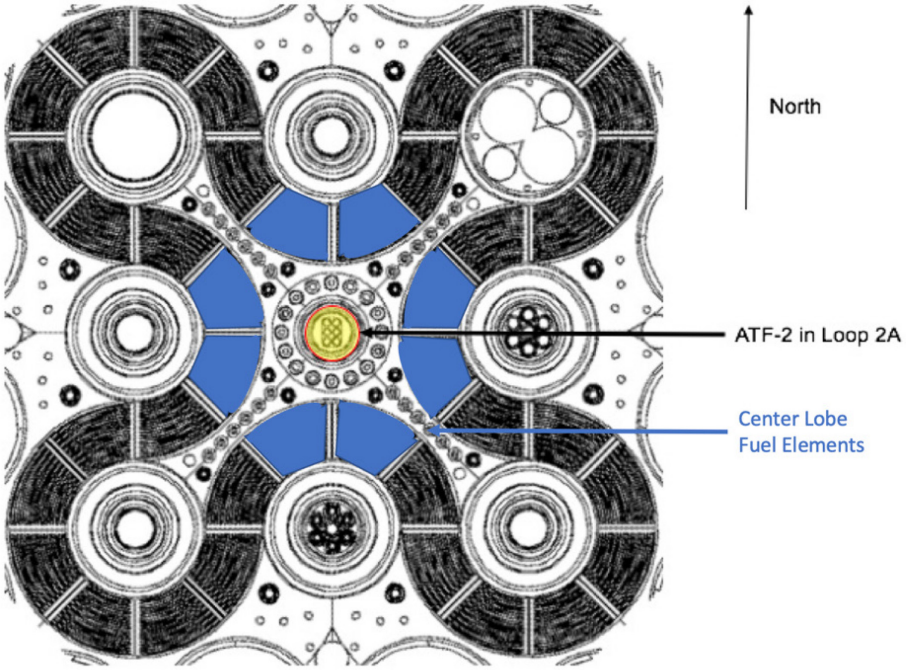

Figure 1. ATR core map highlighting the location of the ATF-2 experiment and center lobe fuel elements.

Of the nine flux traps, six of them house independent pressurized water loops capable of independently supplying pressurized water coolant to the experiments in those positions. Utilization of ATR is shared by the DOE Office of Nuclear Energy and Naval Reactors program. Five of the flux traps (each using a pressurized water loop) are operated for the exclusive use of the U.S. Naval Reactors program to support the continued safe operations of the U.S. nuclear navy. The remaining four flux traps (one outfitted with a pressurized water loop and three employed as multi-purpose positions) and auxiliary testing positions in the beryllium reflector are available for civilian Nuclear Energy research and development. Loop 2A in the center flux trap is currently operating at pressurized water reactor (PWR) conditions with a borated (~1200 ppm) water chemistry and high hydrogen (~50 cc/kg) over pressure. The regular ATF-2 test makes use of this loop during ATR study state cycles and it is proposed to make use of this loop during the transient power cycles for the ATF-2 ramp experiment. The ATF-2 ramp experiment is planned to be inserted in Transient Power Cycle 174A in the late spring/early summer 2024.

2. EXPERIMENT DESIGN

Ramp test rig designs in the R2 and Halden reactors involve a stationary fuel pin in an isolated flow tube. Power in the test pins is manipulated by increasing or decreasing the pressure in a Helium-3 coil or chamber that surrounds the test pin. This approach has the benefit of fine power control and constant axial peaking factors in the test rod during the power ramp. However, a key drawback of this approach is the ability to test only one pin at a time. Both R2 and Halden developed schemes for loading and unloading the ramp test rig while the reactor was still operating to mitigate this drawback. These online shuffling schemes enabled test matrices of the necessary size to test in reasonable time frames. Several operational limitations inhibit the ability of a similar approach to be carried out in the Loop 2A facility at ATR. Thus, INL has developed a test train design that involves the simultaneous ramping of three test pins from a similar CP level to slightly different RTP levels. This test train concept is shown in Figure 2. Rather than using a helium-3 coil, power in the test pins will be controlled using a power axial locator mechanism (PALM) device, which will drive the experiment into and out of the core. These PALM devises are similar to what are used during the transient power cycles at ATR. The ATF-2 ramp test train would be held at a fixed position near the top of the core while NR conducts their PALM testing for the majority of the transient power cycle. Test pin power will be determined by water thermocouples above and below the test pin and the coolant flow rate. The ATF-2 ramp test train would be shielded so that appropriate CP levels will be experienced by the test pins during the high-power phase of NR testing. For example, it is common for center lobe powers to be around 35 MW during the second half of an ATR transient power cycle. It is understood that initially power in the center lobe is a much lower level, ~7 MW for 5 days before moving to ~35 MW for 5 days. In these cases, it is understood that the ATF-2 ramp test pin will undergo a power change from ~50 W/cm to ~250 W/cm. It is also understood that lobe powers can vary by as much as 20% during transient power cycles. Having precise control of the test pin power during the CP part of test is less critical and the ATF-2 ramp experiment will accept these variations.

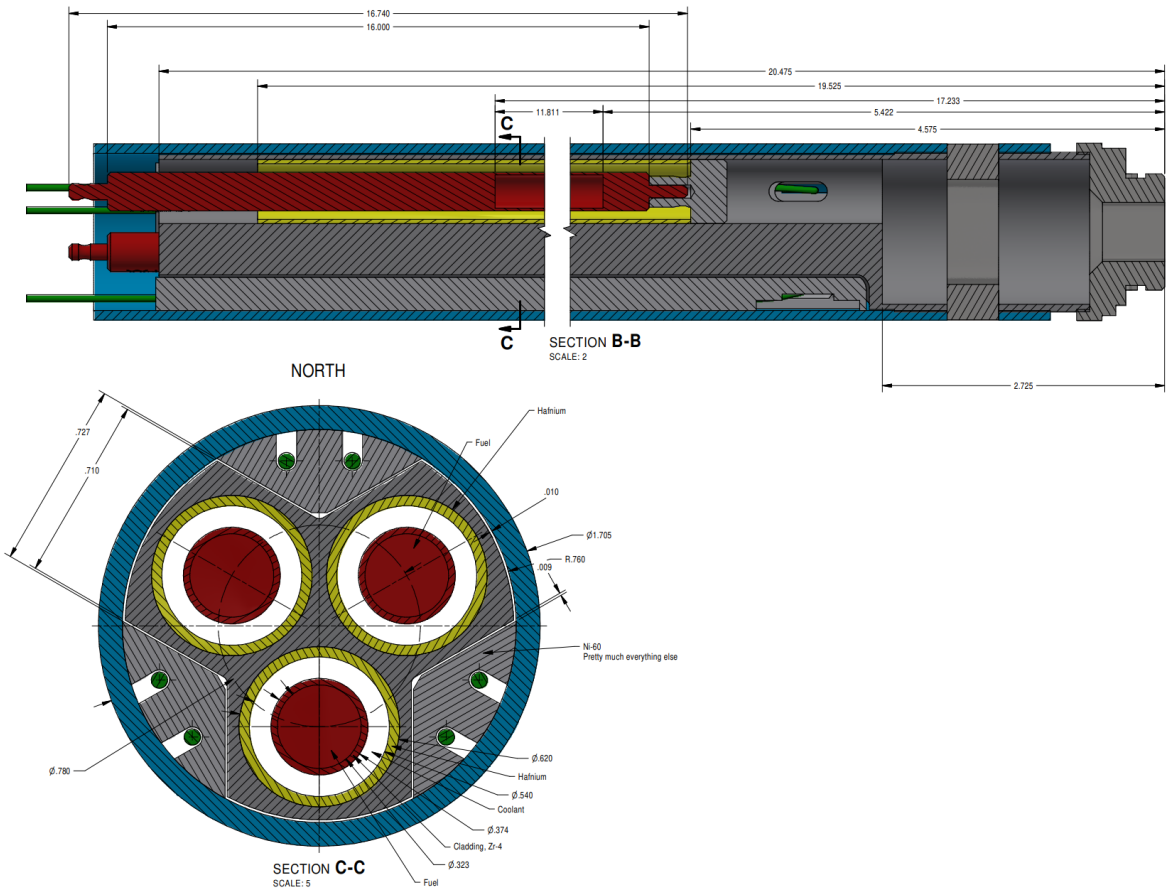

Figure 2. ATF-2 ramp conceptual rendering.

After NR has completed their PALM tests, the ATF-2 ramp test would be inserted to a position near the center of the core (~2.5 ft), increasing test pin power to the RTP level. The test would stay at the RTP level for a minimum of 12 hours before being withdrawn and the reactor shut down. Thus, ATF-2 ramp testing will add only ~1 day to the length of the current PALM cycles. Reactor power during the added day of operation will be the same as during the previous days of operation. While the ATF-2 ramp test is operating at the RTP level, it is important for the reactor power to stay very close to its nominal power level.

Each test pin will be surrounded by a tailored neutron shield shown in green in Figure 3, which will shape the flux around the test pins so that the peak power location will always be somewhere in the center of the test pins, which will be approximately 30 cm in fueled length. The neutron shield will consist of axially stacked concentric rings of either hafnium or zirconium alloys. This will enable different levels of shielding to tailor the flux and thus power in the test pin. This approach also results in a water channel with a constant flow area so as not to upset or overly complicate the thermal hydraulic condition around the test pin.

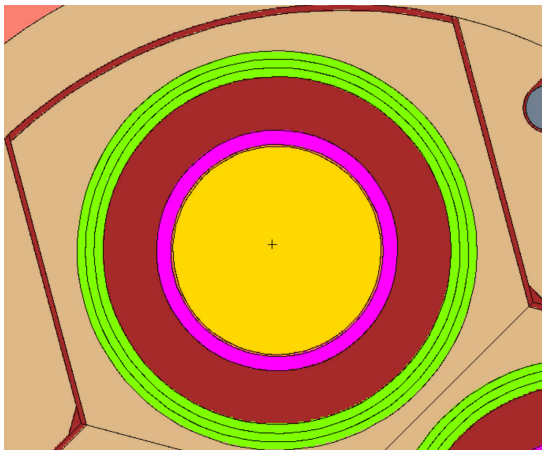

Figure 3. Rendering of neutron shield in ATF-2 ramp test.

Different hafnium shrouds will also cause the power in each pin to be slightly different with the affect being magnified at higher powers allowing for three unique ramp tests to be conducted simultaneously. It is anticipated that that the south facing test pin will have the highest power and will be the lead pin in the experiment. Most tests will be conducted with the lead test pin at or above an anticipated failure limit but with the other two test pins operated below the anticipated failure limit. This will allow failure points to be bracketed and for fuel performance validation data such as fission gas release and test pin permanent hoop strain to be gathered from test pins, which do not fail. Test pins will be outfitted with both a rod elongation attachment and a plenum pressure bellows as shown in Figure 4. Movement of the ferritic cores on these attachments will be observed by and linear variable differential transducer (LVDT) attached to the test hardware although stacking of the ferritic cores only allows rod elongation to be measured in-situ. Rod elongation measurements are deemed more critical for in-situ measurement as these are used to determine the timing of any PCI failures. However, the rod elongation attachment will be designed to be removable such that post-test plenum pressure measurements (and thus a FGR determination) can be made without puncturing of the test pin. It is anticipated that these measurements will be made in the ATR canal following the ramp test along with profilometry measurements to determine the cladding hoop strain and axial gamma scans to confirm the axial peaking factors experienced during the ramp.

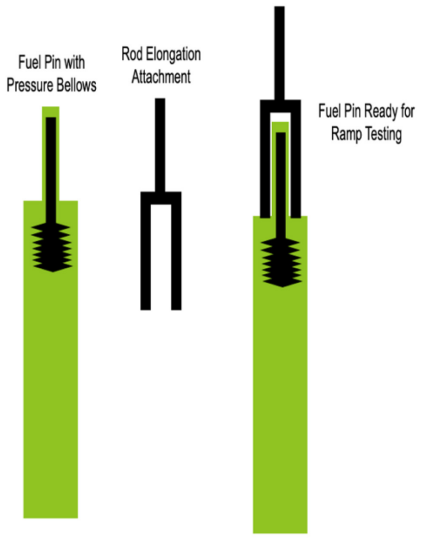

Figure 4. Conceptual test pin design for ATF-2 ramp with an internal pressure bellows and external rod elongation attachment.

3. NEUTRONIC ANALYSIS OF RAMP TEST PERFORMANCE

3.1 Methods

Neutronic performance of the ATF-2 ramp test concept was quantified by Monte Carlo N-Particle Transport Code (MCNP) analysis. The 30-cm fueled portion of the test assembly (Section B-B of Figure 2) was modeled. The ATF-2 ramp test assembly was simulated at six equally spaced elevations in the ATR core.

Table 1. Elevations for neutronic calculations.

Case	Description	Δz of Fuel Bottom from Core Midplane
01	Centered at core midplane	–15.0
02	Bottom at core midplane	± 0.0
03	Centered 30 cm above midplane	+15.0
04	Top at core top	+30.0
05	Centered at core top	+45.0
06	Bottom at core top	+60.0

Cycle 167A was selected as a proxy for the planned test cycle. Cycle 167A is a recent PALM cycle for which driver fuel isotopics and lobe power data are available. Specifically, the **March 13, 21:00** lobe power distribution from Table 2 was used to characterize the MCNP source distribution (Figure 5).

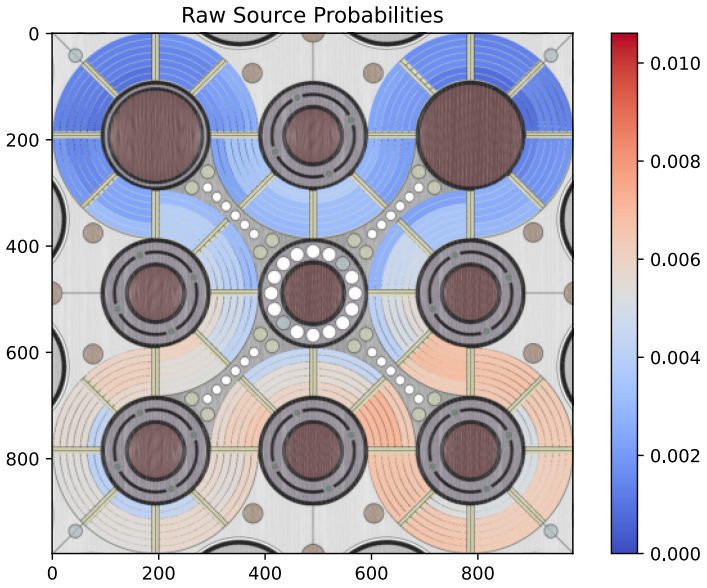

Figure 5. Source distribution assumption.

Table 2. Cycle 167A lobe power history (MW).

Date	NE	SE	SW	NW	C
2020-02-27 19:00	0.43	1.10	1.05	0.50	0.71
2020-02-27 22:00	3.84	9.84	9.43	4.48	6.42
2020-02-28 23:00	4.50	9.22	7.26	5.01	6.66
2020-02-29 16:00	0.01	0.02	0.02	0.01	0.02
2020-03-07 16:00	0.73	1.84	1.77	0.85	1.23
2020-03-07 21:00	3.43	8.58	8.25	4.00	5.71
2020-03-08 21:00	3.16	9.58	7.61	4.75	6.76
2020-03-09 21:00	4.41	10.37	7.17	4.68	7.36
2020-03-10 21:00	4.37	10.24	7.29	4.74	7.33
2020-03-11 21:00	4.37	10.21	7.28	4.74	7.31
2020-03-12 21:00	10.15	23.71	16.65	10.92	16.93
2020-03-13 21:00	16.86	51.31	44.90	18.44	36.71
2020-03-14 11:00	0.00	0.00	0.00	0.00	0.00

Tally results were normalized to a center lobe power of **36.71 MW**. This leads to a lobe-adjusted total core power of around 178 MW and a two-sigma lobe power uncertainty of ±5.4% in all cases. Statistical uncertainty from the Monte Carlo simulation adds no more than ±1%, for a maximum combined two-sigma uncertainty of **±5.5%**.

Several axial and radial variations of the neutron shield design were investigated.

3.2 Conceptual Neutronics Results

The fuel pellet stacks were discretized axially into 29 pellets, and the neutron shields were discretized radially into three equal-volume rings. When multiple shield materials are used, the outer ring is the first

to be changed to hafnium. Coolant is assumed to be at a density of 0.712 g/cm^3 and a boration of 1000 ppm.

3.2.1 All Neutron Shields as Zircaloy-4

Manufacturing the neutron shields out of neutron-transparent materials such as a zirconium alloys shall result in maximum rodlet heating. The linear heat generation rate (LHGR) of the south rodlet peaks at 965 ± 53 W/cm toward the bottom of Case 02.

A small degree of separation between the south (S), northeast (NE), and northwest (NW) rodlet axial heating profiles can be clearly observed at the core midplane. This is caused by the tilted driver fuel flux profile in the PALM cycle (Figure 5). As the experiment elevation increases and the experiment fuel moves further from the core midplane, this separation gradually disappears.

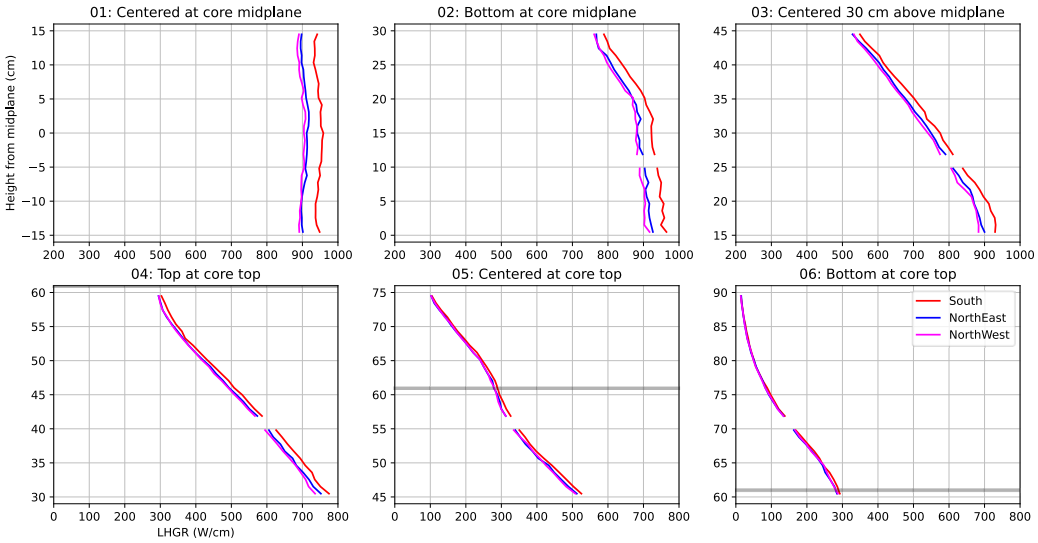

Figure 6. LHGR results with all neutron shields modeled as zircaloy.

3.2.2 All Neutron Shields as Hafnium

Manufacturing the neutron shields out of a strong absorber such as hafnium offers a strong reduction in rodlet heating. The end pellet LHGRs are lowered by over 40%, with an even greater reduction to the heating of the interior fuel pellets.

Considerable end effects are visible at the top and bottom of the power profiles. This is partly a physical phenomenon and partly a symptom of not modeling the neutron shields or full test train above and below the 30-cm fueled portion (refer to Figure 2).

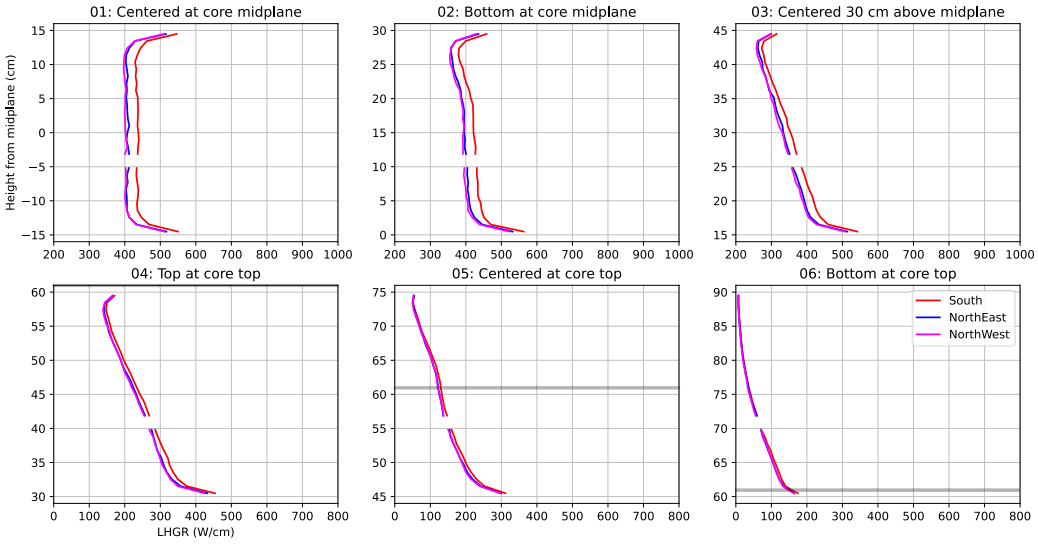

Figure 7. LHGR results with all neutron shields modeled as hafnium.

3.2.3 South Neutron Shield as 2/3 Hafnium

As depicted in Figure 3, the neutron shields can be made to be radially zoned.

Figure 8 shows a design variation identical to the previous one, but with the S neutron shield made 2/3 of hafnium and 1/3 of zircaloy-4. This results in a noticeable increase in the S rodlet LHGR with minimal impact upon the other two.

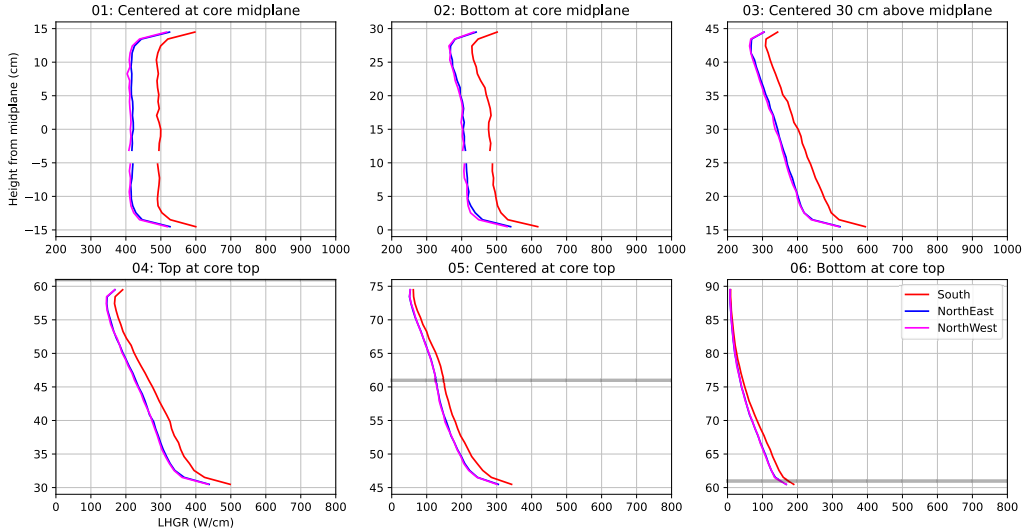

Figure 8. LHGR results with NE and NW neutron shields as hafnium, S as 2/3 hafnium.

3.2.4 South Neutron Shield as 1/3 Hafnium

Figure 9 shows a design variation identical to the previous two, but with the S neutron shield made 1/3 of hafnium and 2/3 of zircaloy-4. This results in further increase in the S rodlet LHGR, while still having minimal impact upon the other two.

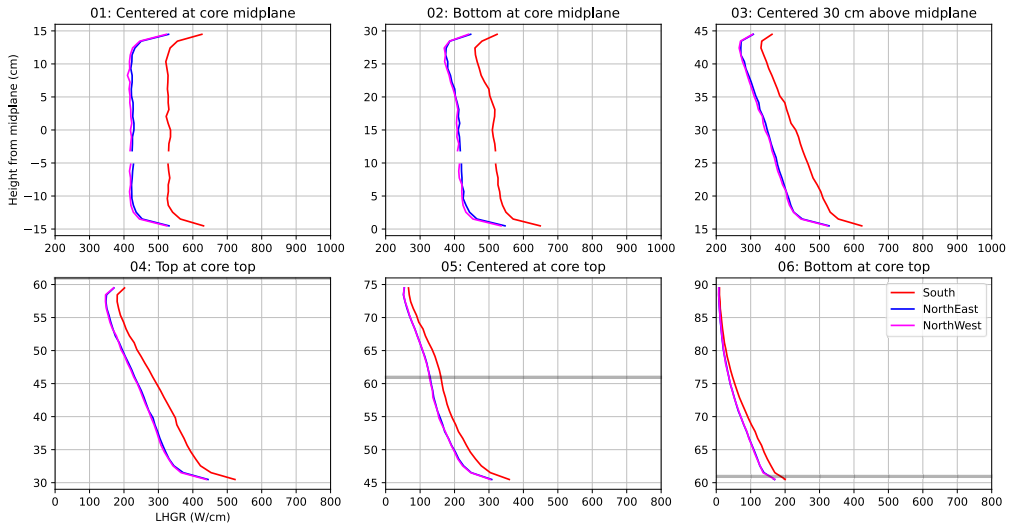

Figure 9. LHGR results with NE and NW neutron shields as hafnium, S as 1/3 hafnium.

3.2.5 South Neutron Shield as Zircaloy

Figure 10 shows a design variation identical to the previous three, but with the S neutron shield made entirely of zircaloy-4. This results in maximum separation between the south rodlet's axial power profile and the two north rodlets' power profile. At core midplane, there is over 100 W/cm difference.

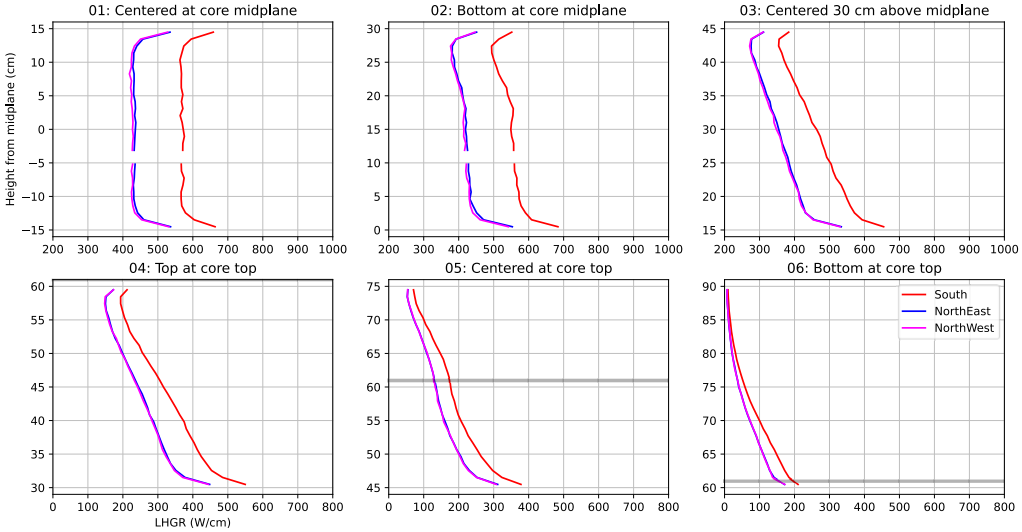

Figure 10. LHGR results with NE and NW neutron shields as hafnium, S as zircaloy.

3.2.6 Reducing End Effects with Buffer Zone

To reduce the marked end effects seen in the previous plots, a buffer zone was placed on either end of the fueled segment. The top and bottom regions of the test train were approximated by 1 cm of hafnium. Figure 11 (below) shows the effects of this buffer on the all-hafnium neutron shield case discussed in Section 3.2.2.

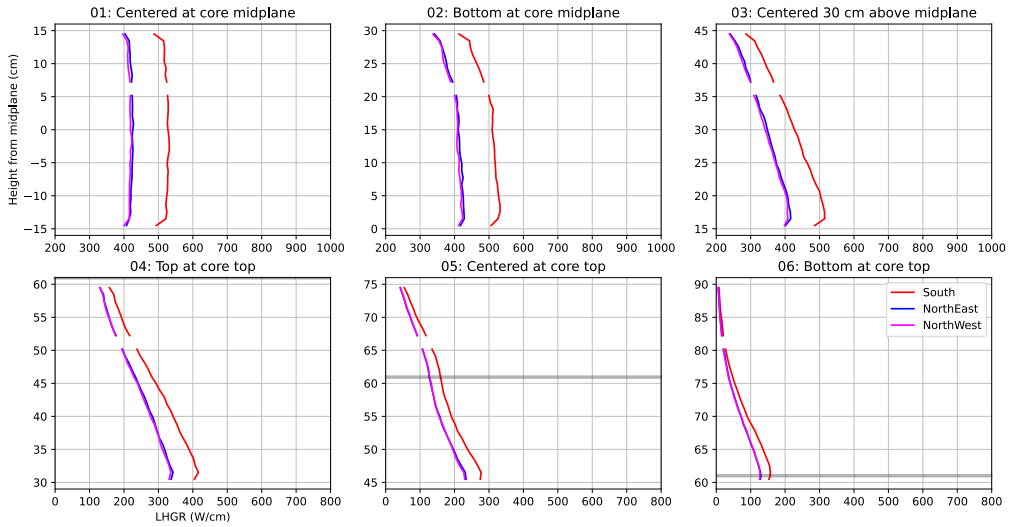

Figure 11. LHGR results with all shields as hafnium (+1 cm axial buffers).

3.2.7 Lower Neutron Shields as 1/3 Hafnium

The neutron shields can be varied axially as well as radially. Figure 12 illustrates the effect of localizing the hafnium to the lower half. All three shields are modeled as 1/3 hafnium, 2/3 zircaloy. The 1-cm hafnium buffer zone is included on either end.

The axially varied design allows ATF-2 ramp to achieve different-shaped power profiles.

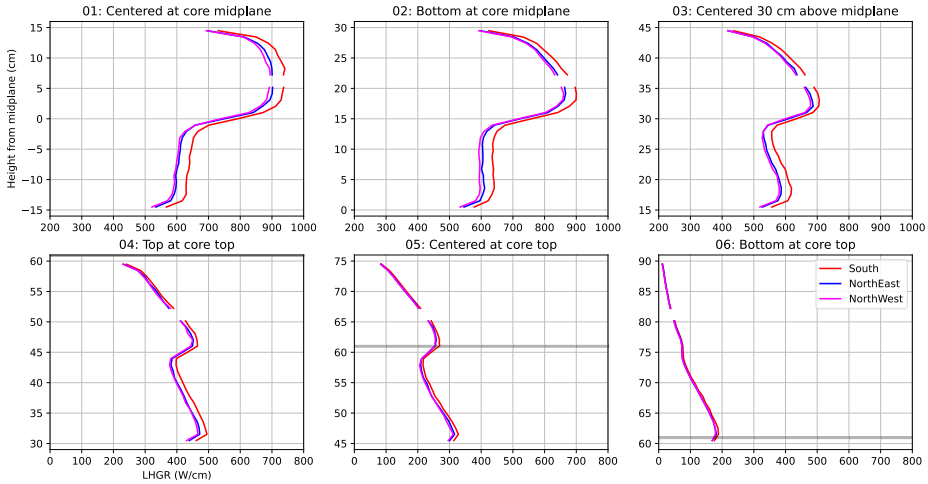

Figure 12. LHGR results with all the lower half of three neutron shields as 1/3 hafnium (+1 cm axial buffers).

3.2.8 Lower Neutron Shields as 2/3 Hafnium

Figure 13 is identical to the previous variation, but with lower half of the three neutron shields modeled as 2/3 hafnium, 1/3 zircaloy. This achieves reduced heat generation in the lower pellets while having almost no effect on the upper ones.

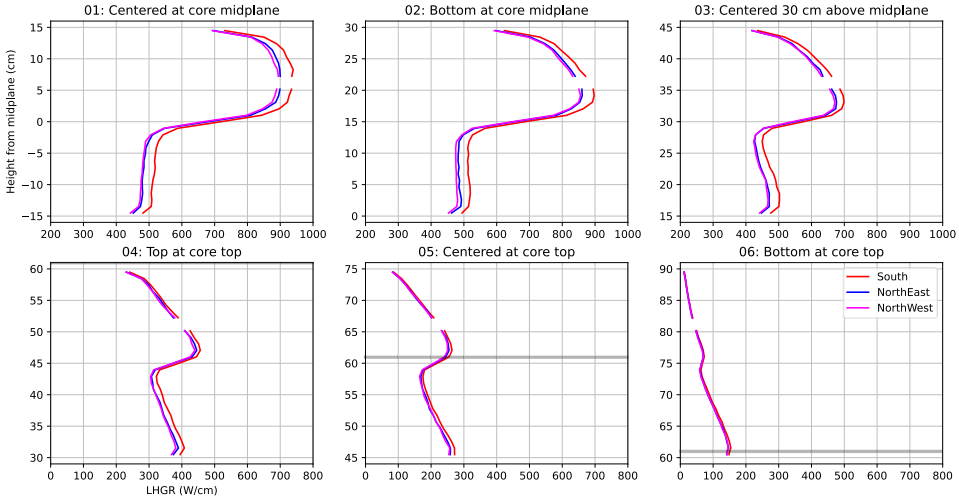

Figure 13. LHGR results with all the lower half of three neutron shields as 2/3 hafnium (+1 cm axial buffers).

3.2.9 Lower Neutron Shields as Hafnium

Figure 14 is identical to the two previous variations, but with lower half of the three neutron shields made entirely of hafnium. This further reduces heat generation in the lower portion while still having minimal effect on the upper portion.

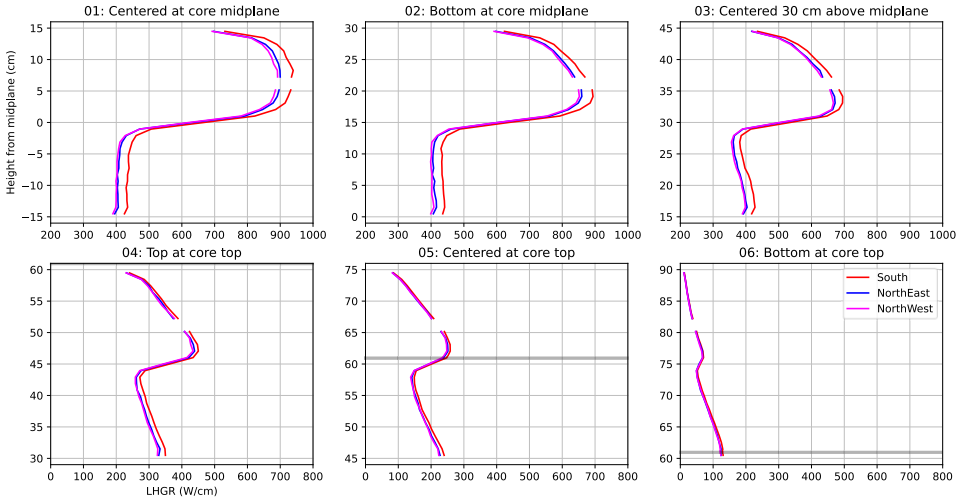

Figure 14. LHGR results with all the lower half of three neutron shields entirely as hafnium (+1 cm axial buffers).

3.2.10 Lower Neutron Shields as Decreasing Thirds of Hafnium

By varying both the radial and axial zones, one can obtain a finer degree of control over ATF-2 ramp's power profiles. Figure 15 demonstrates the effects of using a south lower shield as 1/3 hafnium, 2/3 zircaloy; a northeast lower shield as 2/3 hafnium, 1/3 zircaloy; and a northwest lower shield as all hafnium.

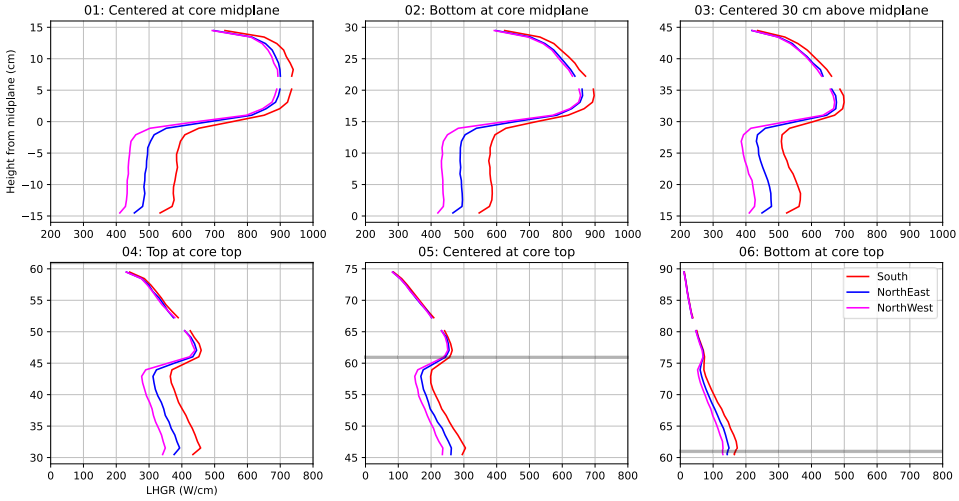

Figure 15. LHGR results with the S, NE, and SW as 1/3, 2/3, and 3/3 hafnium, respectively (+1 cm axial buffers).

3.2.11 Upper and Lower Neutron Shields as Increasing Thirds of Hafnium

Figure 16 shows the effects of varying both the upper and lower shields at the same time. The south rodlet is all zircaloy on the top, with 1/3 hafnium and 2/3 zircaloy on the bottom. The northeast rodlet is

1/3 hafnium and 2/3 zircaloy on top, with 2/3 hafnium and 1/3 zircaloy on the bottom. The northwest rodlet is 2/3 hafnium and 1/3 zircaloy on top, with all hafnium on the bottom. This achieves both rodlet separation and LHGR shaping.

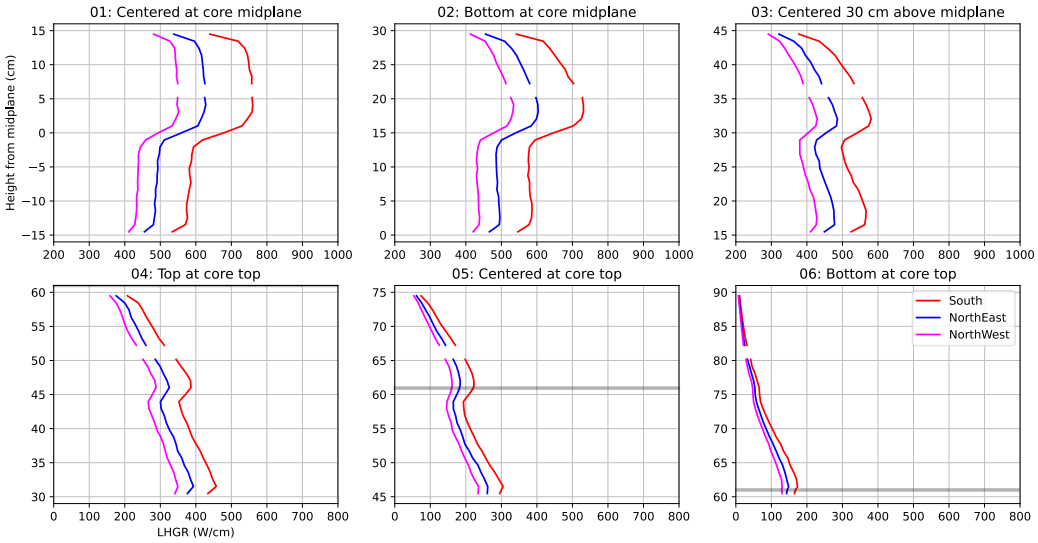

Figure 16. LHGR results with the S as 0/3 and 1/3, the NE as 1/3 and 2/3, and the NW as 2/3 and 3/3 hafnium, respectively (+1 cm axial buffers)

3.3 Neutronic Analysis Conclusions

Given the assumed ATR lobe power distribution and associated uncertainties, a peak LHGR of at least 900 W/cm can be obtained (Section 3.2.1). Power can be reduced to <200 MW by using a PALM device to elevate the fueled region of the ATF-2 ramp test specimen above the ATR driver fuel.

The radial-ring design of the neutron shields grants considerable flexibility in controlling the powers of the three rodlets. Identical adjustments can be made to the three shield (Sections 3.2.1, 3.2.2), much like the shrouds used in steady-state ATF-2 experiments, or they can be adjusted independently to obtain diverging power levels (Sections 3.2.3–3.2.5). The conceptual cases shown here use a binary hafnium-zircaloy split for illustrative purposes, but other combinations of materials are possible. A finer degree of control may also be obtained by varying the number and thickness of the radial zones.

In addition to rodlet and radial variation, this ATF-2 ramp concept can also make use of axial zones to shape the heat generation profile (Sections 3.2.7–3.2.11). Although cases shown here use two axial zones, more zones may be added to the experiment design for yet more control over the power shape.

Overall, the neutronics analysis of the conceptual ramp test design suggest that the combination of axial location and neutron shield design make it possible to obtain the target heating rate values discussed in Section 2.